Proceedings of the DIS'2004, Štrbské Pleso, Slovakia

QUARK-ANTIQUARK EXCHANGE IN $\gamma^* \gamma^*$ HIGH ENERGY SCATTERING

MICHAEL LUBLINSKY
DESY Theory Group, DESY
Notkestr. 85, 22607 Hamburg, Germany
E-mail: lublinm@mail.desy.de

Some results on the high energy behavior of quark-antiquark exchange in $\gamma^* \gamma^*$ elastic scattering are presented. The ladder diagrams provide a perturbative QCD model for secondary reggeon.

$\gamma^* \gamma^*$ collisions at high energies provide a unique laboratory for testing asymptotic properties of pQCD. The dominant contribution to the process is given by the BFKL Pomeron which gives rise to a cross section strongly rising with energy.

At present, the only source for experimental data on $\gamma^* \gamma^*$ collisions is LEP. It has become clear that at LEP energies, the cross section is not yet dominated by the pomeron. The data rather indicate the necessity to include several corrections. An important class of corrections is due to secondary reggeons which denote the exchange of mesons. In virtual $\gamma^*\gamma^*$ scattering we may expect that such secondary exchange may become accessible to a perturbative analysis, similar to the BFKL. The meson exchange is modeled by the exchange of $q\bar{q}$ ladders [1].

Due to appearance of double logs the cross section goes as $\sim s^{\omega_0 - 1}$ with the intercept of the order $\omega_0 = \sqrt{4\lambda} = \sqrt{2\,\alpha_s\,C_F/\pi} \simeq 0.5$. It is remarkable that this intercept obtained in pQCD is very close to the nonperturbative one known from the Regge phenomenology. In [4] a detailed study of the high energy behavior of quark-antiquark exchange in $\gamma^*\gamma^*$ scattering in the double logarithmic approximation was performed. We present here several results from [4].

The lowest order diagram for the scattering amplitude $T^{\gamma^*\gamma^*}$ of the elastic $\gamma^*\gamma^*$ scattering process is a quark box (we take the virtualities of external photons to be equal): $p_A^2 = -Q^2\,;\quad p_B^2 = -Q^2\,;\quad (p_A + p_B)^2 = s\,;\quad x = Q^2/s\,.$ The Sudakov decomposition $k = \beta q - \alpha p + k_\perp$ with the light cone vectors p, q defined through $p_A = p - x\,q\,;\quad p_B = q - x\,p\,;\quad p^2 = q^2 = 0\,;\quad 2\,(p\,q) = s\,.$ The expression for the box diagram (in the high energy approximation) is proportional to

$$\int_x^1 \frac{d\beta}{\beta} \int_{max(\mu_0^2,\,\beta\,Q^2)}^{\beta\,s} \frac{dk^2}{k^2}, \tag{1}$$

The first energy log then comes from the β integration. As to the remaining integral over the transverse momentum, it is the fermionic nature of the exchanged particles which provides, in the trace in the numerator, the additional k^2 factor and thus renders the momentum integral logarithmic. We have introduced the infrared cutoff μ_0^2 below which pQCD cannot be trusted. Depending on external kinematics we distinguish two regions + (hard) and −. The result for the box diagram is

$$T^{\pm}_{box} \;=\; \tau_{TT} \left\{ \begin{array}{ll} \ln^2 \frac{s}{Q^2} & if \quad \mu_0^2 \;<\; \frac{Q^4}{s} \\ \ln^2 \frac{s}{Q^2} - \frac{1}{2}\left(\ln \frac{s}{Q^2} - \ln \frac{Q^2}{\mu_0^2} \right)^2 & if \quad \frac{Q^4}{s} \;<\; \mu_0^2 \end{array} \right\}. \tag{2}$$

The total cross section for $\gamma^* \gamma^*$ follows from

$$\sigma^{\gamma^* \gamma^*} \;=\; \frac{1}{s} Im\, T \;\simeq\; \frac{1}{s} \frac{\pi\, \partial T}{\partial \ln s} \tag{3}$$

(with the last approximate equality being valid in the high energy approximation).

$$\sigma^{\gamma^* \gamma^*}_{Born} \;=\; \tau_{TT}\, \pi \left\{ \begin{array}{lll} 2\, \ln \frac{s}{Q^2} & if & \mu_0^2 \;<\; \frac{Q^4}{s} \\ \ln \frac{s}{\mu_0^2} & if & \frac{Q^4}{s} \;<\; \mu_0^2 \end{array} \right\}. \tag{4}$$

It is easy to generalize this analysis to the case of unequal photon masses, $Q^2_{1,2}$. In this case the boundary of the hard domain is given by $Q_1^2\, Q_2^2 \;=\; \mu_0^2\, s$.

We turn to higher order corrections described by the QCD ladder diagrams [3,2,6,5]. Each i-th rung in the ladder contributes $\lambda \int \frac{d\,\beta_i}{\beta_i} \int \frac{d\,k_i^2}{k_i^2}$. The double logarithms arise from the following ordering:

$$x \;<\; \beta_1 \;<\; \beta_2 \;<\; ... \;<\; \beta_{n-1} \;<\; \beta_n \;<\; 1; \quad Q^2 \;<\; \frac{k_n^2}{\beta_n} \;<\; \frac{k_{n-1}^2}{\beta_{n-1}} \;<\; ... \;<\; \frac{k_1^2}{\beta_1} \;<\; s\,.$$

In addition we require for each rung to satisfy $k_i^2 \;>\; \mu_0^2$. Fig. 1 illustrates the Bethe-Salpeter type equation we are deriving for the sum of ladder diagrams. We remove the lower s-channel quark line coupling; in this way we obtain the elastic amplitude A for the photon-quark scattering.

$$A(\beta,\, k^2) \;=\; 1 \;+\; \lambda \int_{Q^2/s}^{\beta} \frac{d\beta'}{\beta'} \int_{max(\beta'\, k^2/\beta\;,\; \mu_0^2)}^{\beta'\, s} \frac{dk^{'2}}{k^{'2}}\, A(\beta',\, k^{'2})\,. \tag{5}$$

The limits of integration follow from the above kinematic ordering. As in the case

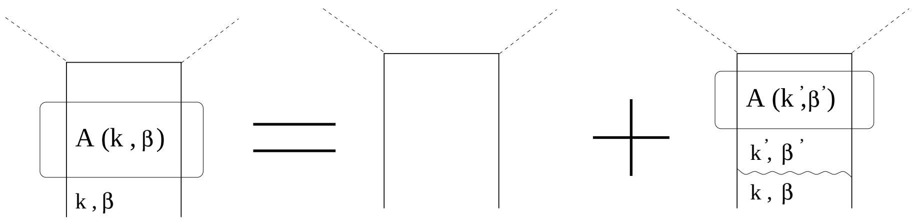

Figure 1. The Bethe - Salpeter equation.

of the box diagram we distinguish between two regions I_A^+ and I_A^-:

$$A^+(\beta,\, k^2) = 1 + \lambda \int_{Q^2/s}^{\beta} \frac{d\beta'}{\beta'} \int_{\beta'\, k^2/\beta}^{\beta'\, s} \frac{dk^{'2}}{k^{'2}}\, A^+(\beta',\, k^{'2}); \quad I_A^+ :\; \mu_0^2 < \frac{Q^2 k^2}{\beta\, s} \tag{6}$$

$$A^-(\beta,\,k^2) \;=\; 1 \,+\, \lambda \int_{Q^2/s}^{\beta} \frac{d\beta'}{\beta'} \int_{\beta'\,\mu_0^2/Q^2}^{\beta'\,s} \frac{dk'^2}{k'^2}\, A^+(\beta',\,k'^2) \tag{7}$$
$$+\,\lambda \int_{Q^2/s}^{\beta\,\mu_0^2/k^2} \frac{d\beta'}{\beta'} \int_{\mu_0^2}^{\beta'\,\mu_0^2 s/Q^2} \frac{dk'^2}{k'^2}\, A^-(\beta',\,k'^2)$$
$$+\,\lambda \int_{\beta\,\mu_0^2/k^2}^{\beta} \frac{d\beta'}{\beta'} \int_{\beta'\,k^2/\beta}^{s\,\beta'\,\mu_0^2/Q^2} \frac{dk'^2}{k'^2}\, A^-(\beta',\,k'^2)\,; \qquad I_A^- \,:\; \frac{Q^2\,k^2}{\beta\,s} \,<\, \mu_0^2\,.$$

The amplitudes T for the photon-photon scattering is obtained from A by subtracting the terms $A_0 = 1$, putting $k^2 = Q^2$ and $\beta = 1$. The full scattering amplitude is obtained by adding the twisted (with respect to $s \leftrightarrow u$ crossing) fermion loop.

In the hard region I_A^+, Eq. (6) can be brought to the form

$$\frac{d^2 A^+}{d\xi\,d\eta} \;=\; \lambda\,A^+\,; \qquad \eta \;=\; \ln(\beta\,s/Q_1^2); \qquad \xi \;=\; \ln(\beta\,s/k^2)\,. \tag{8}$$

This is a wave equation in the light cone coordinates. Its solution is given by $A^+(\xi,\,\eta) \;=\; I_0\left(\sqrt{4\,\lambda\,\xi\,\eta}\right)$. We skip the expression for A^- in the infrared sensitive region I_A^-. Define $\omega_0 \;=\; \sqrt{4\,\lambda}$; $\tilde{Q}^2 = \sqrt{Q_1^2\,Q_2^2}$. Then

$$T^+ = T(Q_1^2,\,Q_2^2,\,s) = \frac{4\tau_{TT}}{\omega_0^2}\left[I_0\left(\omega_0\sqrt{\ln\frac{s}{Q_1^2}\ln\frac{s}{Q_2^2}}\right) - 1\right] \;\; if\;\mu_0^2 < \frac{\tilde{Q}^4}{s} \tag{9}$$

$$T^- = T(Q_1^2,\,Q_2^2,\,s) \;=\; \frac{4\,\tau_{TT}}{\omega_0^2}\;\times$$
$$\left[I_0\left(\omega_0\sqrt{\ln\frac{s}{Q_1^2}\,\ln\frac{s}{Q_2^2}}\right) \,-\, 1 - \frac{\ln\frac{s\,\mu_0^2}{\tilde{Q}^4}}{\ln\frac{s}{\mu_0^2}}\, I_2\left(\omega_0\sqrt{\ln\frac{s\,\mu_0^2}{\tilde{Q}^4}\,\ln\frac{s}{\mu_0^2}}\right)\right] \tag{10}$$

Let us consider the $s \to \infty$ asymptotics. In the region $1 \ll s/\tilde{Q}^2 \ll \tilde{Q}^2/\mu_0^2$, the asymptotics is obtained from the behavior of the Bessel function I_0

$$T^+(s \to \infty) \;=\; \frac{4\,\tau_{TT}}{\omega_0^2\,\sqrt{2\,\pi\,\omega_0\,\ln(s/\tilde{Q}^2)}}\left(\frac{s}{\tilde{Q}^2}\right)^{\omega_0}, \tag{11}$$

In the region $\tilde{Q}^2/\mu_0^2 \,\ll\, s/\tilde{Q}^2$ the leading asymptotics cancel. We obtain:

$$T^-(s \to \infty) = \frac{8\,\tau_{TT}}{\omega_0^2\sqrt{2\pi}(\omega_0\ln(s/\tilde{Q}^2))^{3/2}}\left(\frac{s}{\tilde{Q}^2}\right)^{\omega_0}\left[1 + \omega_0 \ln\frac{\tilde{Q}^2}{\mu_0^2} + \frac{\omega_0^2}{4}\ln^2\frac{\tilde{Q}^2}{\mu_0^2}\right] \tag{12}$$

The power behavior in s is the same in both regions. The difference lies in the preexponential factors: in the second region, we have a slightly stronger logarithmic suppression, and there is a logarithmic dependence upon the infrared scale μ_0^2.

It is instructive to compare our results for the high energy behavior of quark-antiquark exchange in $\gamma^*\,\gamma^*$ scattering with those for gluon exchange, i.e. the LO BFKL Pomeron. For the latter it is well-known that when energy grows, diffusion in $\ln k^2$ broadens the relevant region of internal transverse momenta, which has the shape of a "cigar" (Fig. 2a). Its mean size is of the order $\sqrt{\ln s}$

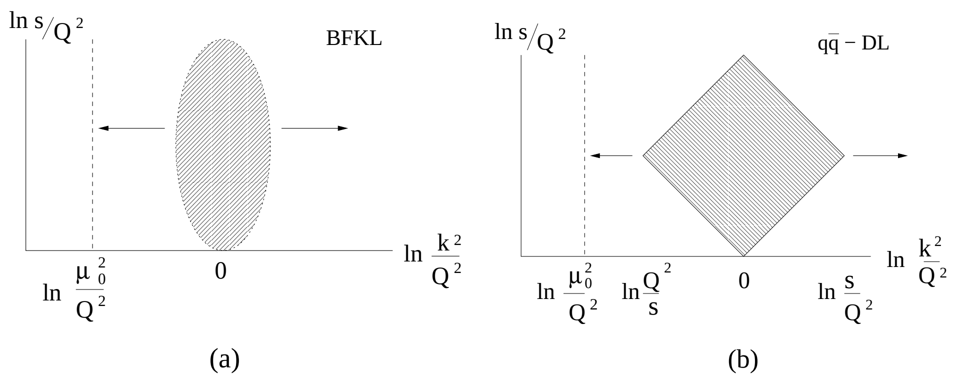

Figure 2. Energy dependence of the region of integration in a) BFKL and b) quark ladder.

and eventually reaches the infrared cutoff μ_0^2. We can make an analogous analysis of quark-antiquark exchange. Since internal transverse momenta range between $max(Q^4/s,\, \mu_0^2) \;<\; k^2 \;<\; s$ or, equivalently $max(-\ln s/Q^2,\, \ln \mu_0^2/Q^2) \;<\; \ln k^2/Q^2 \;<\; \ln s/Q^2$, there is, for not too large energies, a limited region where transverse momenta stay above the infrared scale, and the use of pQCD is justified. With increasing energy, the k^2-region expands and eventually hits the infrared cutoff μ_0^2. In order to understand, in the fermion case, the region of internal integration in more detail, consider the amplitude A^+ (Fig.1). It satisfies the two dimensional wave equation (8) which can be rewritten as

$$\left(\frac{\partial^2}{\partial t^2} - \frac{\partial^2}{\partial z^2} - 4\lambda\right) A^+ \;=\; 0; \qquad t \;=\; \ln\frac{\beta s}{\sqrt{k^2 Q^2}}; \qquad z \;=\; \frac{1}{2}\ln\frac{k^2}{Q^2}.$$

Let us confront this with the BFKL Pomeron: in Fig.2b we have drawn the square ("diamond") which illustrates the internal region of integration. In the fermion case its width in $\ln k^2$ grows proportional to $\ln\, s/Q^2$, i.e stronger than in the BFKL case where $\ln\, k^2$ grows as $\sqrt{\ln\, s/Q^2}$.

The author is very grateful to Jochen Bartels for the fruitful collaboration.

References

1. M.G. Ryskin and A.G. Shuvaev, *Eur. Phys. J.* **C 25** 245 (2002).
2. V. G. Gorshkov, V. N. Gribov, L. N. Lipatov and G. V. Frolov, *Sov. J. Nucl. Phys.* **6** 95 (1968), [*Yad. Fiz.* **6**, 129 (1967)]; *Sov. J. Nucl. Phys.* **6** 262 (1968), [*Yad. Fiz.* **6** 361 (1967)].
3. R. Kirschner and L. N. Lipatov, *Nucl. Phys.* **B 213** 122 (1983). *Sov. Phys. JETP* **56** 266 (1982), [*Zh. Eksp. Teor. Fiz.* **83** 488 (1982)].
4. J. Bartels and M. Lublinsky, *JHEP 0309* 076 (2003); hep-ph/0406273.
5. B. I. Ermolaev, S. I. Manaenkov and M. G. Ryskin, *Z. Phys.* **C 69** 259 (1996).
6. J. Kwiecinski, *Phys. Rev.* **D 26** 3293 (1982);
   R. Kirschner, *Z. Phys.* **C 31** 135 (1986); ibid **C 67** 459 (1995).